Infectious DNA clone technology and inoculation strategy for Rose Rosette Virus that includes all seven segments of the negative-strand RNA genome.

Mingxiong Pang[a], Mathieu Gayral[a], Kelsey Lyle[c], Madalyn K. Shires[d], Kevin Ong[d], David Byrne[b], Jeanmarie Verchot[a1]

[a]Texas A&M Agrilife Center in Dallas, 17360Coit Rd, Dallas TX 75252

[b]Department of Horticulture Sciences, Texas A&M University, College Station, TX 77843

Department of Biological Sciences, University of Texas at Dallas, Dallas TX 75252

[d]Department of Plant Pathology & Microbiology, Texas A&M University, College Station, TX 77843

[1] corresponding author: Jeanmarie Verchot, Texas A&M Agrilife Center in Dallas, 1736 Coit Rd, Dallas TX 75252 phone: 972-952-9224; email: jm.verchot@ag.tamu.edu

Author Contributions: MP, DB, JV designed research; MP, KL, MS performed research; MP, DB, KO, MG, and JV analyzed data; MP, DB, MG, KO and JV wrote the paper.

Keywords: Reverse genetic system, Emaravirus, plant virus, infectious clone,

The authors declare no conflict of interest

Abstract

The ability to mutate the genomic nucleic acid of viruses is the most straight-forward approach to understanding virus genetics. Reverse genetics of RNA viruses involves the introduction of mutations at the cDNA level, and then introducing cDNAs into cells to produce infectious progeny virus. Reverse genetic tools are used to investigate the products of viral genes, virus-host interactions relating to pathogenicity and immunity, and requirements for vector transmission. The technology has been slow to develop for viruses with negative strand RNA genomes and has been especially difficult for plant viruses with multicomponent negative strand RNA genomes, many of which require an insect vector for transmission to be successful. *Rose rosette virus* (RRV; Emaravirus) is a negative-sense RNA virus with a 7-segmented genome that is enclosed by a double membrane (1-4). We devised a technology for delivery of plant sap inoculum which can also deliver agrobacterium containing infectious clones to rose plants. We report the first reverse genetic system for a member of the Emaravirus genus, Rose rosette virus (RRV). We introduced fluorescent proteins at three locations in the seven segmented genome and learned that such reporters can be stably maintained during systemic infection. This study demonstrates that RRV can infect Arabidopsis causing significant growth alterations of the plant, while causing mild to more serious disease symptoms in *Nicotiana benthamiana* and two varieties of roses. This reverse genetic system creates new opportunities for studying negative strand RNA viruses infecting plants.

Significant Statement

Since an infectious clone for influenza virus was developed in 1998, little progress has been made in infectious clone technology for viruses with negative strand genomes. We constructed an infectious clone of the seven-segmented RRV genome that is contained in a binary vector and delivered by Agrobacterium. RRV has emerged as a serious threat to cultivated roses, causing millions of dollars in losses to commercial producers. This technology is a game changer for investigations into Emaravirus genetics, studies of molecular virus-host interactions, as well as for rose breeders who can use the infectious clone for rapid germplasm screening to identify useful resistance for breeding programs.

INTRODUCTION

Among the most significant technological advances for research into virus life cycles has been the development of cDNA copies of viral genomes that can be reverse transcribed to produce infectious virus (5). This technology enables the genetic manipulation of cDNA for reverse genetic analysis of the virus life cycle, and for investigations into the molecular basis of virus-host interactions for susceptibility and immunity. The infectious cDNA technology was rapidly adopted for studying positive strand RNA viruses. Since exact 5' ends are critical for launching the first round of translation and replication of transcripts to generate infectious virus genomes, plasmids and infectious cDNA inserts are often combined with bacteriophage T7,

SP6, RNA pol I, or RNA pol II promoters fused to the exact 5' end of the virus genomic cDNA (6-11). Exact 3' ends are also critical and so transcriptional terminators or hepatitis delta virus ribozymes are often located at the 3' ends to produce transcripts with exact 3' ends (7, 8, 12-14). The second advance in infectious clone technology was the discovery that genetic sequences encoding foreign peptides, large proteins, and small noncoding RNAs can be integrated into specific locations of viral genomes and these recombinant virus clones can be used as tools for reverse genetics of their hosts, for overexpression of peptides and proteins that can be purified for vaccine production or other purposes (15-23). Among plant RNA viruses, green fluorescent protein (GFP) and derivatives, or iLOV genes have been incorporated into viral genomes (24). Combining visual markers of infection with reverse genetic technology has been a powerful combination for functional imaging to uncover critical roles for viral proteins in the virus life cycle. These combined technologies have also been central to discovery of molecular plant-virus interactions occurring in susceptible hosts or that govern gene-for-gene resistance.

Infectious clone technology has been slower to develop for viruses with negative strand RNA genomes because the naked genomic or antigenomic RNAs are not able to initiate infection by themselves. The minimum infectious unit for this type of virus requires a ribonucleoprotein (RNP) complex composed of viral genomic RNA and RNA dependent RNA polymerase (P proteins). Among negative strand RNA viruses, the first infectious clones were produced for viruses with non-segmented genomes belonging to the families *Rhabdoviridae*, *Paramyxoviridae, and Filoviridae* (Ebola) (25-29). Generally, infection is achieved by delivering viral genomic cDNAs that produce transcripts that function as anti-genomic RNAs (agRNA). Plasmids encoding the nucleocapsid core or subunits of the viral polymerase are co-delivered with the agRNA encoding cDNAs that successfully spur the replication process. The first infectious clone of a negative strand RNA virus that infects plants was *Sonchus yellow net virus* (SYNV) (6, 7, 25, 30). The SYNV full-length cDNA was introduced into a binary vector fused to a duplicated Cauliflower mosaic virus 35S promoter. Additional binary plasmids expressing the N (nucleocapsid) protein, P (phosphoprotein) and L (polymerase) protein are co-delivered with the viral cDNA plasmid by agroinfiltration to plant leaves to produce active SYNV infection.

The first infectious clone of influenza A virus, which has eight genome segments, was reported in 1999 based on the transfection of *in vitro* constituted RNP complexes (31, 32). The eight genome segments are produced using a promoter that depends upon the cellular RNA pol I for synthesis of agRNA alongside four plasmids that expressed proteins required for viral

replication and transcription (PB1, PB2, PA, NP). More recent infectious clones have been developed which consist of several plasmids providing bidirectional expression of viral RNAs from RNA pol I and pol II promoters for reverse genetic studies in transfected eukaryotic cells (33).

Here we report an infectious clone of *Rose rosette virus* (RRV), a member of the Emaravirus family that has seven genome segments (34). Roses are the economically most important ornamental plants belonging to the family *Rosaceae*. RRV has been devastating roses and the rose industry in the USA, causing millions of dollars in losses (35). Typical symptoms of RRV include rapid stem elongation, breaking of axillary buds, leaflet deformation and wrinkling, bright red pigmentation, phyllody, and hyper-thorniness (36, 37). Currently researchers rely on viruliferous eriophyid mites to deliver RRV to plants, and mechanical delivery of RRV to test plants has not been demonstrated to be consistently effective. Here we developed a mechanical delivery method using homogenate inoculum, and this technology can also be used for delivery of an infectious clone by agrobacterium. To produce infectious clone, each cDNA is located next to the duplicated CaMV 35S promoter to produce an exact 5' end and a 3' hepatitis delta virus ribozyme (HDR) to generate an exact 3' end. We successfully introduced the green fluorescent protein (GFP) and iLOV reporter protein genes in three locations to determine the best location in the genome for adding new genetic features. This enhanced visual reporter system for the infectious clone will be useful for screening rose germplasm stocks for new sources of resistance.

Results

Mechanical inoculation of *Arabidopsis thaliana* and *Nicotiana benthamiana* using RRV containing naturally infected rose sap

Currently researchers rely on viruliferous eriophyid mites to deliver RRV to plants, and mechanical delivery of RRV to roses has been described as unreliable. For many viruses that can only be transmitted by an insect or other type of vector, mechanical inoculation of an infectious clone cannot be easily achieved. Therefore, a critical step toward developing an infectious clone was to devise a method for mechanical inoculation of rose plants and we chose to use naturally infected rose sap for this stage of work. We prepared homogenate inoculum by grinding leaf tissue from naturally infected roses ('Julia Child') in 0.05 M phosphate buffer (pH 7.0)(1:30 w/v). We added RNase inhibitor and 0.1% volume of Silwet-77 to the extract and loaded to the reservoir of a pressurized artist airbrush. The soluble leaf homogenate was

applied to *Arabidopsis thaliana*, *Nicotiana benthamiana* and roses plants that were dusted with carborundum (Fig. 1A). The leaves were harvested for diagnostic testing after 6 days, and plants were generally maintained for up to 60 days to monitor infection.

RT-PCR was used to detect the production of RRV transcripts in inoculated leaves, as evidence that the sap inoculations resulted in productive infection. Diagnostic RT-PCRs produced the expected size fragments between 104 and 600 bp (Fig 1B and Table S1) and confirmed the accumulation of virus transcripts representing the seven segments in *A. thaliana* and *N. benthamiana* leaves. Representative PCR products representing RNA1, RNA5, RNA6 and RNA7 from samples of *A. thaliana, N. benthamiana* and rose leaves were sequenced. Multiple sequence alignment using CLUSTALW confirmed that the PCR products were RRV transcripts. Data compiled from multiple experiments (Table 1) showed that virus infection was detected in 72% (13/18) and 100% (12/12) of sap-inoculated *Arabidopsis and N. benthamiana* plants, respectively, by 6 days post inoculation (dpi) (SI Appendix, Methods).

To further demonstrate that RRV can be mechanically inoculated to plants using an artist airbrush, we used the dsRNA binding-dependent fluorescence complementation (dsRBFC) assay, consisting of FHV B2, to detect RRV dsRNAs, which accumulate as replication intermediates, in *N. benthamiana* leaves. The two FHV B2 dsRNA binding domains fused to N- and C-terminal halves of YFP were introduced into binary plasmids and delivered by *Agrobacterium* into RRV inoculated and mock-inoculated *N. benthamiana* leaves. Binding by B2 proteins to common dsRNAs brings the two halves of YFP together and produced visible yellow fluorescence (38) throughout the epidermal cells of RRV infected leaves taken from four plants but was not reconstituted in mock-inoculated leaves (Fig 1C). The combined results of RT-PCR and dsRBFC confirm that RRV can successfully infect *A. thaliana,* and *N. benthamiana* following mechanical inoculation. These data establish that RRV infection can be established in host plants without requiring a population of viruliferous mites to establish infection. These data also identified two alternative host for RRV.

Construction of functional infectious clone of RRV and mechanical inoculation to rose plants

To prepare the RRV infectious clone, the full-length cDNAs for agRNA1 (7026 bp), agRNA2 (2245 bp), agRNA3 (1544 bp) and agRNA4 (1541 bp) were synthesized *do novo* and inserted into the small binary plasmid pCB301-HDV, which contains the double CaMV 35S promoter, HDV antigenomic ribozyme, and Nos terminator (25). Plasmids were named

pCB301-agRNA1, -agRNA2, -agRNA3, and -agRNA4. Then cDNAs encoding the agRNA5 (1665 bp), agRNA6 (1402 bp), and agRNA7 (1649 bp) were directly amplified through RT-PCR using total RNA isolated from infected rose leaves, and then introduced into the pCB301-HDV backbone creating pCB301-agRNA5, -agRNA6, and -agRNA7 plasmids. The antigenomic cDNA positioned next to the CaMV 35S promoter and HDRz to produce viral transcripts with authentic 5' and 3' ends (Fig. 2). All constructs were confirmed by sequencing before being transformed into *A. tumefaciens*.

Agrobacterium cultures were combined in equal ratios and we inoculated two cultivars of roses ('The Knock Out'® and 'The Double Knock Out'®) with all seven clones encoding RRV antigenomic segments (RRV1-7) using an artist airbrush. We monitored plants, especially the new emerging branches and leaves, for symptoms for 48 days. Systemic infection was detected in new emerging leaves using the diagnostic agRRV4-F1/R1 primer set (Table 1). Between 30 and 40 dpi, 88 -100% of plants became systemically infected. Pictures were taken at 48 dpi. The foliar symptoms were different between the two cultivars. The upper non-inoculated leaves of 'The Knock Out'® roses tested positive for virus infection but showed no symptoms (Fig 3A, B). At 48 dpi 'The Knock Out'® roses did not show any signs of witch's broom, which is the characteristic symptom for rose rosette disease. 'The Double Knock Out'® roses showed early signs of witch's broom (Fig. 3C-G). The internode length was smaller than the healthy plants. The leaves were rounder and misshapen and this exposed the thorniness of the plants. Apical buds and the stem showed necrotic patches. We conducted diagnostic RT-PCR (Table 1) and genome segment specific RT-PCR to confirm systemic infection (Suppl. Fig. 1). Diagnostic RT-PCRs produced the expected size fragments between 104 and 600 bp (Fig 3B and Table S1) and confirmed the accumulation of virus transcripts representing the seven segments. These data were surprising because it is commonly accepted that to initiate infection from cDNA clones encoding antigenomic RNAs of negative strand RNA viruses requiring adding plasmids expressing the viral replicase, viral nucleocapsid, and viral glycoprotein, as well as viral encoded RNA silencing suppressors *in trans* (7).

Agro-delivery of infectious clones to Arabidopsis produces successful infection and unexpected disease phenotypes

The first report of RRV genome sequence identified four segments and then a subsequent report identified three additional segments (2, 3). From these reports it is not clear whether the first four segments are the essential elements for infection, or if all seven segments are essential. We analyzed the coding sequences of each RNA segment in both orientations

and determined each to be monocistronic. InterPro was used to search for proteins with similar sequences to the predicted translation products of each viral RNA. The results indicate that RNA1 encodes a protein that is 2276 amino acids in length and likely functions as the viral RNA dependent RNA polymerase. RNA2 encodes a protein that is 645 amino acids in length and is predicted to be the membrane glycoprotein to encapsulate the virus genome. RNA3 encodes a 319 amino acid length protein that is predicted to be the nucleocapsid, and RNA4 encodes a 361 amino acid protein that is predicted to be the movement protein (Table S2). Each RNA5, RNA6 and RNA7 are predicted to be monocistronic and InterPro searches carried out using the predicted translation products did not reveal any putative functions for these proteins (Table S2). These results led us to investigate whether RNAs1 through 4 were sufficient to achieve systemic infection or if all seven RNA segments are essential.

Agrobacterium cultures were combined in equal ratios and then infiltrated to twenty-three-day old *A. thaliana* (Col-0) plants that were grown in short day length (10 h light and 14 h dark, 23°C) (Fig. 3). We determined that agroinfiltration technology works well for delivery of infectious clones to these plants, although it does not seem effective for delivery to roses. Four to six plants were inoculated with the combination of RRV segments 1, 2, 3 and 4 (RRV1-4) or the combination of RRV segments 1 through 7 (RRV1-7) and experiments were repeated 3 times. Control plants were agroinfiltrated to deliver an empty pCB301 plasmid (Mock). For Arabidopsis, RT-PCR was carried out at 25 dpi to detect RNA4 related transcripts in the upper non-inoculated leaves confirming that the plants became systemically infected (Table 1). The pooled data showed that the majority of plants inoculated with RRV1-4 or RRV1-7 became infected (Table 1). These data confirmed our expectations that RNA1-4 contain the essential features for successful infection.

We also noted that Arabidopsis plants produced a disease phenotype that is different from roses. Arabidopsis inflorescences emerged in mock treated plants around 59 days after germination while among plants inoculated with RRV1-4 or RRV1-7, the inflorescences emerged much earlier, at 45 days (Fig. 3). Plant height from the soil surface to the top of the inflorescences were measured for all plants at 68 days after germination (45 dpi) and the average height for mock treated *A. thaliana* plants was 22.0 cm (Table 2). Plants infected with RRV1-4 or RRV1-7 were taller than mock treated plants, ranging in height from 45-51 cm (Fig. 3A, Table 2). Conventional RT-PCR verified the presence of RRV1-4 or RRV1-7 in plants that were measured (Fig. 3B). The RRV1-4 or RRV1-7 inoculated leaves primarily displayed

symptoms that were mild yellow mottling which was not seen on the mock treated and untreated leaves (Fig. 3C).

The plant structure was altered by infection. After bolting, mock inoculated plants produced three inflorescence stems with five to six cauline leaves and a solitary flower (Fig. 3A and 3D; Table 2). All plants infected with RRV1 -4 or RRV 1-7 produced the three major inflorescences with multiple leaves and higher order branches with a greater abundance of flowers (Fig. 3A and 3E, Table 2). Plants infected with RRV1-7 showed more basal leaves in the vegetative rosette than mock-inoculated plants and RRV1-4 infected plants (Fig. 3F). RRV1-4 and RRV1-7 infected plants showed an abundance of aerial rosettes that form at the axils where cauline leaves normally develop, suggesting that virus infection alters the developmental patterning of axillary meristems (Fig 3G and H; Table 2). The number of siliques on mature infected plants at 45 dpi was 4- to 5-fold greater than on mock treated plants (Table 2). Virus infected plants produced more seed than mock treated plants. The 1000 seed weight for mock treated plants was 16 mg, while RRV1-4 and RRV1-7 infected were 17 mg and 18 mg respectively. Seeds were collected from plants, and 120 seeds were germinated on ½ MS media and 100 % of the seeds germinated producing plants.

Agro-delivery of infectious clones to *N. benthamiana* produces successful infection

Among the *N. benthamiana* plants inoculated with RRV1-4 or RRV1-7, 75-85% were confirmed by RT-PCR to be systemically infected within 25 dpi (Table 1). Plants symptoms at 20-25 dpi varied widely from mild to severe yellow mottling (Fig. 4A, 4B and 4C). We conducted individual RT-PCR to verify the presence of each RNA segment or, multiplex RT-PCR to simultaneously detect all seven RNA segments (Fig. 4D and 4E)(SI Appendix, Methods). To demonstrate that equal amounts of RNA were used for RT-PCR analysis, we used primers to detect EF1 in *N. benthamiana* and Actin in roses as internal controls (Table S1) and loaded equal volumes of PCR products in each lane to show similar amplicon levels among each sample (Fig. 4D). The PCR products representing RNA segments 1 through 4 varied between samples. Fig 4D shows two representative samples that demonstrate the appearance that the viral RNAs do not accumulate to equivalent levels in infected leaves within a single infected plant. We also noted the levels of virus accumulation in systemic leaves of the same age can vary significantly between plants. PCR products detecting RNA1 often produced lower product accumulation than did RNA2, RNA3 and RNA4 (Fig. 4D) using these primer sets. In another set of experiments, we employed the aatbRRV F/R primer set (Table S1) that recognizes the conserved 5' and 3' sequences of all seven RNAs that produce amplicons of all seven RNAs in

single multiplex reaction (Fig. 4E). Similar primer sets were reported in Babu et al (2016) to produce intermediate length and full length amplicons (3). In these experiments (Fig. 4E), all RNAs were readily detected in plants infected with RRV1-4 or RRV1-7. In this case full length amplicons corresponding to RNA2 were not always abundant between samples. There were intermediate size amplicons of 1.8 and 2.0 kb which are likely derivatives of RNA 2 as reported in Babu et al (2016). The genomic RNAs 3 and 4 are 1544bp and 1541 bp respectively, RNA6 is 1402 bp, and the RNA5 and 7 are 1655bp and 1649 bp respectively. The resulting PCR products representing RNAs3-7 co-migrate on an agarose gel (Fig. 4E).

Among the *N. benthamiana* plants that were inoculated with RRV1-4 (Table 1), the two samples in Fig. 4D were selected to analyze for the presence of RRV dsRNAs using RNAse protection assays (39). These were chosen because one sample produced low levels of PCR products and the second sample generated 5- to 10- fold more product (Fig. 4D and F). Amplicons ranging from 500 to 585 bp were generated indicating double strand RNAs 1, 2, 3 and 4 are present in infected *N. benthamiana* plants but not in the mock treated plants (Fig 4F). RNA from infected rose plants from field samples produced similar RNAs 1-4 amplicons while none were detected in healthy rose samples (Fig. 4E).

To further verify that these *N. benthamiana* plants were infected with RRV, we prepared sap inoculum using (1:30 w/v) 0.05 M phosphate buffer (pH 7.0) and leaves from a *N. benthamiana* plant infected with RRV1-7 at 25 dpi. This sap was used to inoculate six Arabidopsis plants (6-leaf stage) using an artist airbrush (SI Appendix, Methods). RT-PCR was done at 25 dpi using RNA extracted from upper non-inoculated leaves of the Arabidopsis plants and two of the six inoculated plants tested positive for RRV infection (Table 1).

Stable expression of GFP-P4 fusion protein during RRV infection

The ability to engineer GFP into the recombinant cDNAs encoding viruses has been powerful for studying virus cell-to-cell and systemic movement in plants. The GFP gene was introduced into RNA4 as a fusion to the P4 open reading frame (Fig. 5A) to determine if this infectious clone could be tagged with a visual marker to track virus movement. Plants were infiltrated with RRV1-4 or RRV1-7 using the GFP containing construct (named 4R4-GFP or 7R4-GFP). Experiments were repeated 3-5 times using *Arabidopsis* and *N. benthamiana* plants. While 50% of Arabidopsis plants became infected with 4R4-GFP or 7R4-GFP, all *N. benthamiana* plants became systemically infected (Table 1). The infected *N. benthamiana* plants showed necrotic regions on the inoculated leaves at 12 dpi, and throughout the upper

leaves as the virus continued to spread systemically (Fig. 5A). By 35 dpi, virus- infected plants showed significant systemic yellowing and necrosis, while mock treated plants remained green (Fig. 5A). GFP was not obvious when observing under a hand-held UV lamp, however, we could easily detect GFP using an epifluorescence microscope (Fig. 5B). GFP-P4 fusions may not be a useful visual reporter for whole plant studies, especially if the fusion is the cause of necrosis, but may be suitable for microscopic imaging to track P4 proteins in infected cells. Immunoblot analysis was used to confirm the GFP fusions in 4R4-GFP and 7R4-GFP inoculated plants. We detected the abundant ~70 kDa fusion protein in upper non-inoculated leaves at 19 dpi (Fig 5C). Diagnostic RT-PCR using agRRV4-F1/R1 primer set that detects a 500 bp fragment of RNA4 was done to verify that the plants were infected (Fig. 5D; Table 1). To further confirm that all RNA segments spread systemically, we conducted RT-PCR, to detect each genome segment as in Fig. 5. Representative gels in Fig. 5E demonstrate that in each experiment where plants were inoculated with the infectious clone combining four or seven segments, they became systemically infected with all segments. We used the agRRV4-F1 and smeGFP-R primers to detect a 1266 bp band for RNA4. Notably we sometimes observed 2 bands overlapping the GFP sequence in RRV-4 which raises the possibility that GFP may not be stable and there may be some recombination within this segment (Fig. 5E).

iLOV-based fluorescent reporter introduced into RRV genome

The iLOV protein is a fluorescent flavin based domain of the plant blue light receptor, phototropin (24). The iLOV is a photoreversible fluorescent protein that is an excellent alternative to GFP for tracking virus infection (24). We introduced iLOV into the RRV genome fused to the ORF2 (Fig 6A). *N. benthamiana* plants were inoculated with RRV-4R2-iLOV and RRV-7R2-iLOV (Fig. 6B). All plants were systemically infected by 25 dpi and produced yellow mottling symptoms on infected leaves. The P2-iLOV fusion seemed less necrotic to the plant than P4-GFP fusion during RRV infection. Epifluorescence microscopy detected the iLOV fusion proteins in epidermal cells at 13 dpi (Fig. 6B). The iLOV coding sequence was also introduced into RNA5, replacing the ORF5 sequence (Fig. 6A, C). Plants were infiltrated with RRV-7R5-iLOV and systemic mottling and necrosis symptoms were evident at 25 dpi (Fig. 6C). Epifluorescence microscopy also detected the iLOV fusion proteins at 13 dpi in the upper non - inoculated leaves (Fig. 6D). Diagnostic RT-PCR using the agRRV4-F1/R1 primer set was performed to verify that the plants were infected (Fig. 6D). As with the prior experiments, we conducted additional RT-PCR to detect each genome segment confirming systemic infection (Fig. 6E). We used the agRRV2-F1 and R2_iLOV-R primers to detect a 1080 bp band for RNA2

that overlaps the fused viral and iLOV sequences. We used IF-agR5_F and iLOV-R primer pair to detect the iLOV sequences in RNA5 and this produced a 433 bp band (Fig. 6E). Both RNA2 and RNA5 can support infection with the iLOV insertion. The amplicon RNA5-iLOV is more abundant than the RNA2-iLOV (Fig. 6E).

DISCUSSION

An infectious virus clone from a cDNA copy of the viral genome is a powerful tool for reverse genetic studies of any virus. For viruses with negative strand RNA genomes, infectious clones of several bunyaviruses infecting mammals (27, 40) have been reported but there has been limited progress in developing such technology for plant infecting viruses (7). The main limitation is that the naked RNA is not itself transmissible and infectious without the inclusion of the viral nucleocapsid protein (34). In 2015, there was a breakthrough in the production of an infectious virus from cloned *Sonchus yellow net virus* (SYNV) cDNAs. The strategy was to clone the full-length viral genome encoding cDNA into binary vectors next to the 35S promoter and provide the nucleocapsid (NC) and replication factors on separate plasmids (7, 25, 26). Success in this system required the co-delivery of the viral replicase as well as several viral silencing suppressor proteins to reduce the effects of the cellular silencing machinery while galvanizing the initial replication steps (6, 7, 26). There is also a breakthrough in developing a reverse genetic system for tospoviruses by the Tao Xiaorong lab (personal communication). Here we report the first infectious clone of a member of the *Emaravirus* genus of multipartite negative strand RNA virus, a breakthrough technology establishing a reverse genetic system for RRV. This technological advance is remarkable because the plasmids containing viral antigenomic cDNAs that produce infection without providing the viral replicase, NC proteins or silencing suppressor proteins on separate plasmids. The ability to deliver these plasmids to roses using the airbrush or to Arabidopsis and N. benthamiana by agro-infiltration was not expected since RRV is reported to be only transmissible by a mite vector (37, 41). This opens new possibilities for molecular characterization of plant emaraviruses and adds to the established tools needed by virologists and rose breeders to combat infection. This new technology is important to accelerate up the process of identifying genes conditioning resistance to the virus that can be introgressed into new rose cultivars.

RRV is the most devastating viruses of roses in North America. The disease and its symptoms were described in the 1940s and it was first described as a virus with a negative-

sense RNA genome in 2011 (2). Initially, RRV was reported to have 4 genomes segments. RNAs 5, 6 and 7 were identified and sequences were reported in NCBI between 2014 and 2016 (3). Here we report the first-generation binary RRV infectious clones that produce all seven RNA segments. RNA segments 1-4 were derived from sequences provided in NCBI. The segments of RNAs 5-7 were PCR amplified from infected roses. We demonstrate that the infectious clone produces significant changes to the structure of Arabidopsis plants, while producing chlorotic and mild symptoms in *N. benthamiana* during the 60 days that we monitored infection. The two rose cultivars showed different symptoms, with the Double Knockout presenting early evidence of witch's broom disease. The effects of RRV on Arabidopsis plant growth, branching, and silique development makes this reverse genetic system a powerful tool for studying how viruses can alter the plant development programming. This is valuable because reports by rose breeders and gardeners identify rose plants that are infected with RRV to have excessive thorns and witches' broom. The onset of these disease symptoms from the time of inoculation is not known and it is possible that it may take more than one season to see these changes in an outdoor garden (36, 41). This new infectious clone technology will also enable investigators to monitor the progression of disease in susceptible host plants and learn more about how RRV changes rose plant development over multiple seasons. Because we can see rapid changes in the plant architecture of Arabidopsis, we can begin to study the changes in plant developmental programming using the RRV infectious clone as a virus-host model system to inform genetic studies in roses. This new powerful technology will accelerate the development of roses resistant to RRV.

This study used two technologies to detect viral dsRNA and confirm successful infection of plants by mechanical inoculation with sap or infectious clones. The first assay using dsRNA binding-dependent fluorescence complementation technology in live plant tissue. Yellow fluorescence was seen in virus infected but not mock inoculated leaves. RNAse protection assay was also used to verify the accumulation of RRV1-4 in systemically infected leaves (38, 39). Early studies of negative-strand RNA viruses reported that the viral RNA-dependent RNA polymerase produces little or no dsRNAs as replicative intermediates in most of these viruses (42). However more recently, dsRNA production was detected using immunofluorescence antibody staining in *Vesicular stomatitis virus* (VSV), *Measles virus* (MeV), *Influenza A virus* (IAV) and *Nyamanini virus* (NyaV) which all belong to different families with negative strand RNA genomes (43). With RRV, dsRNA accumulation is mainly in the cytoplasm although higher resolution microscopic studies are needed to determine if there is any pattern of nuclear

accumulation. While the dsRNA detection technology used in this study is not specific for RRV, excluding other possible sources of infection or cellular dsRNAs, the results obtained here including the mock treated plants, show a correlation between RRV infection and dsRNA detection *in vivo*. The RNAse protection assays detected RRV dsRNAs that were recovered from infected plants using PCR primers to amplify only RRV templated molecules, and this provides more specific verification that infection produced systemic dsRNA as a cellular product of the viral RNA-dependent RNA polymerase.

We introduced GFP and iLOV proteins into three locations of the RRV genome to contrast the effects of inserting heterologous genes on virus infection and host symptoms. There appears to be no change in virus accumulation or delay in systemic spread when the infectious clones harbored either the GFP or iLOV genes. However, the pattern of symptoms was altered by each insertion, although the infectious clones with the iLOV insertion caused milder symptoms than did the infectious clone with the GFP insertion, suggesting that the nature and position of the fluorogenic reporter could influence virus protein activities. It was interesting to see that the infectious clone with the P2-iLOV fusion or the insertion replacing the P5 gene produced mild yellowing and occasional minor necrosis in *N. benthamiana* plants, while the P4-GFP fusion changed the disease pattern, turning leaves necrotic. This result suggests that P4, which is already identify as a putative movement protein in the *Emaravirus* family (Table S2), could also have an anti-necrotic function. We noted that a reduced number of Arabidopsis plants became infected with the 4R4-GFP or 4R7-GFP compared to infectious clones containing the iLOV gene, suggesting that the P4-GFP fusion could also reduce virus movement ability. The P2 of *Emaravirus* is a glycoprotein with unknow function as P5 (Table S2). The P2-iLOV fusion and P5 replacement seems to be less disturbing for the virus cycle since RRV-RNA2-iLOV and RRV-RNA5-iLOV infectious clone induce less necrose than the RRV-RNA4-GFP infection. We also noticed that on occasion, PCR amplification of GFP produced two bands while the iLOV always produced a single band. It is worth speculating that GFP may be a less stable insert and that the smaller bands were the result of recombination within the viral RNA. The iLOV protein is smaller than GFP and for that reason maybe more easily incorporated into the genome. However, although both were visible using a microscope, neither of these fluorescent proteins could be seen using a hand-held UV lamp. Thus, more investigations are needed to develop a second-generation infectious clone that contains a visible reporter of infection that is less necrotic and easily visible using a hand-held lamp.

Finally, our research found that rose plants are difficult to agro-infiltrate. We were able to overcome this obstacle to virus delivery by using an artist airbrush. Using this delivery system, we were able to introduce the RRV1-7 infectious clone to rose plants. Plants were observed for more than 45 days to confirm infection and we noted that different rose cultivars show different diseases patterns and susceptibility.

In summary, we established a new infectious clone technology for plant infecting negative strand RNA viruses that can be broadly used for reverse genetic studies and for breeding programs to characterize rose germplasm for virus resistance. The most significant and surprising outcomes was that this infectious clone system does not require additional plasmids containing replication factors to galvanize the replication cycle. We cannot answer why this the case for this virus, but we are initiating new investigations of virus replication in isolated plant protoplasts to gain new information about emaravirus replication . We established dsRNA detection technology for detecting RRV infection in cells that are enriched for viral sequences. We demonstrated that iLOV may be a better reporter of infection than GFP. Future efforts will be made to improve the infectious clone technology for expression of heterologous protein expression and further establish this new robust reverse-genetic system. This technology opens the possibility to begin to screen rose plants for new sources of resistance that can be used in future breeding programs.

Materials and Methods

Construction of RRV infectious clones

All plasmids were maintained in *Escherichia coli* DH5α cells and in *Agrobacterium tumefaciens* strain GV3101. Synthesized full-length cDNAs of the antigenomic (ag)RNA sequences for RRV segments 1 through 4 (NCBI reference sequences NC_015298.1, NC_015299.1, NC_015300.1, and NC_015301.1) were prepared and inserted into pUC57 and pCB30-HDV plasmids by GenScript (Piscataway, NJ). The pCB301-HDV plasmid is a binary plasmid with a duplicated cauliflower mosaic virus (CaMV) 35S promoter and 3' hepatitis delta virus ribozyme (HDRz) sequence which was provided by Dr Zhenghe Li (Zhejiang University, Hangzhou China). The full length agRNA segments 5, 6 and 7 (MN095111,MN095112, MN095113) were amplified by RT-PCR prepared from infected rose leaves (var 'Julia Child') using the following primer pairs: IF_agR5F/R, IF_agR6F/R, and IF_agR7F/R (Table 1) with 15 nt that overlap vector sequences (Table 2).

To introduce smeGFP (MN095110) into the RRV genome, unique *Stu*I and *Sma*I restriction sites (aggcctcccggg) were engineered into the 3' end of RRV_R4 ORF at 1167-1669 in pCB301-RNA4. Single molecule GFP (smeGFP) was PCR amplified from a TRV-smeGFP plasmid using the smeGFP_F/R primer pair containing S*tu*I and S*ma*I restriction sites (Table 1). Linearized vectors and PCR products were ligated to generate pCB301-R4-smeGFP. To prepare pCB301_R2 iLOV and pCB301_R5 iLOV constructs, the primers of R2_iLOV.F/R with pCB301_R2.F/R and R5_iLOV.F/R with pCB301_R5.F/R (Table 1) were used to amplify iLOV fragments from TMV_iLOV (24) and fragments of pCB301_R2 and pCB301_R5. All PCRs were carried out using high-fidelity 2X Platinum SuperFi® Green PCR Master Mix (Invitrogen). The high fidelity directional In-Fusion® HD Cloning Kit (Takara Bio USA, Inc.) was used to introduce each amplified full-length cDNA into the pCB301-HDV.

Plant materials and virus inoculation

Arabidopsis thaliana plants were grown in at 23°C with a 10 h/14 h (day/night) photoperiod in a growth chamber. *Nicotiana benthamiana* were grown at 23°C with 16 h/ 8 h (day/night) photoperiod in a growth chamber. Rose plants were grown in a greenhouse with temperature settings to at 23°C. Three-weeks-old plants were inoculated with extracts taken from rose rosette virus infected rose plants (var. Julie Child). Plant extracts were prepared by grinding 0.5 g infected leaves in 15 mL (1:30 w/v) 0.05 M phosphate buffer (pH 7.0) and filtered through cheesecloth. Then SUPERaseIn™ RNase inhibitor (Invitrogen) (1 U/ml) and 0.1% volume of Silwet-77 were added to the extract and loaded to the reservoir of an artist airbrush. Plants were lightly dusted with carborundum and extracted leaf homogenate was applied using the Central Pneumatic® ¾ an 3 oz airbrush kit (Harbor Freight, Plano TX) (Fig. 1A).

Three-weeks-old plants were also infiltrated with *A. tumefaciens* cultures harboring constructs for each RRV agRNA segment. Cultures were grown overnight in YEP media, resuspended in MES buffer (10 mM $MgCl_2$, 10 mM MES, pH 5.6, and 150 uM acetosyringone), and adjusted to an optical density A_{600} of 1.0. After a 2-4 hours of incubation in the dark, equal volumes of each *Agrobacterium* culture were mixed at 1.0 OD and loaded to a 1 ml syringe for infiltration to *N. benthamiana* and *Arabidopsis*. Mixed *Agrobacterium* cultures were delivered to rose plants using the Central Pneumatic® air brush.

dsRNA binding-dependent fluorescence complementation (dRBFC), RT-PCR and, RNaseI protection assays

The dsRNA binding-dependent fluorescence complementation assay was performed according to Cheng et al (2015) (38). *Agrobacteria* expressing B2-YN and B2-YC (Addgene) were mixed in equal amounts and directly infiltrated into *N. benthamiana* leaves that were inoculated with RRV containing sap and control leaves that were treated with buffer only. The YFP fluorescence was visualized using a Nikon Eclipse 90i epifluorescence microscope.

Total RNA was extracted from the upper leaves of plants infiltrated with the infectious clone using the Maxwell® 16 Instrument LEV simplyRNA Purification Kits (Promega). All reverse transcription reactions were carried out using random primers and the High-capacity cDNA reverse transcription kit (Applied Biosystems®). PCR amplification was performed using GoTaq® G2 master mixes DNA polymerase (Promega) with the following primer pairs: agRRV1-F1/R1, agRRV2-F1/R1, agRRV3-F1/R1, agRRV3-F2/R2, agRRV4-F1/R1, agRRV5-F1/R1, agRRV5-F1/R1, agRRV6-F1/R1 and agRRV7-F1/R1 (Table 1). We used primer pairs to detect Actin and EF1 transcripts (44) in Arabidopsis and *N. benthamiana* and roses as internal controls for RT-PCR verification of virus infected plants (Table 1)

RNaseI protection assays were performed using total RNA (5 ug) from *N. benthamiana* leaves, as well as infected or healthy rose leaves from field samples according to (39). Samples were treated with DNase I for 1 h at 37°C. RNase I-treated RNA was reverse transcribed using random primers and then amplified using the following primer pairs: agRRV1-F1/R1, agRRV2-F1/R1, agRRV3-F2/R2 and agRRV4-F1/R1 (Table 1). All PCR amplified products were subjected to 1.2% agarose gel electrophoresis stained with ethidium bromide (39).

Immunoblot detection of plant viruses

Total proteins were extracted from healthy and systemically infected *N. benthamiana* leaves using extraction buffer (100mM Tris-HCl, pH6.8, 2.5%SDS, 100mMDTT, 100 mMNaCl and 10% glycerol). Proteins were separated on 4–20% Mini-PROTEAN® TGX™ Precast Protein Gels (Bio-Rad) and then transferred to PVDF membranes using the Trans-Blot Turbo System (Bio-Rad). Blots were probed with HRP-conjugated GFP-tag mouse monoclonal antibody (Proteintech, Rosemont IL). Membranes were also monitored for equal loading by staining with Ponceau S or Coomassie blue.

Epifluorescence microscopy

Leaves were examined with a Nikon Eclipse 90i epifluorescence microscope using the FITC (Fluorescein Isothiocyanate) filter (excitation 465nm/495nm; emission 515nm/555nm) to detect YFP, GFP and iLOV. Images were captured using a DS-Ri1 camera and NIS-Elements AR-3.2 software (Nikon).

Acknowledgements

Dr. Li Zhenghe from Zhejiang University for providing the pCB301-HDV plasmid for our constructions. Michele Scheiber at Star Roses and Plants for providing rose liners for experiments. The American Rose Society for providing financial gift that enabled this research. USDA's National Institute of Food and Agriculture (NIFA) Specialty Crop Research Initiative project "Combating Rose Rosette Disease: Short Term and Long-Term Approaches" (2014-51181-22644/ SCRI).

References

1. Mielke-Ehret N, Mühlbach HP. 2012. Emaravirus: a novel genus of multipartite, negative strand RNA plant viruses. Viruses 4:1515-36.
2. Laney AG, Keller KE, Martin RR, Tzanetakis IE. 2011. A discovery 70 years in the making: characterization of the Rose rosette virus. J Gen Virol 92:1727-32.
3. Babu B, Washburn BK, Poduch K, Knox GW, Paret ML. 2016. Identification and characterization of two novel genomic RNA segments RNA5 and RNA6 in rose rosette virus infecting roses. Acta Virol 60:156-65.
4. Di Bello PL, Ho T, Tzanetakis IE. 2015. The evolution of emaraviruses is becoming more complex: seven segments identified in the causal agent of Rose rosette disease. Virus Res 210:241-4.
5. Ahlquist P, French R, Janda M, Loesch-Fries LS. 1984. Multicomponent RNA plant virus infection derived from cloned viral cDNA. Proc Natl Acad Sci U S A 81:7066-70.
6. Qian S, Chen X, Sun K, Zhang Y, Li Z. 2017. Capped antigenomic RNA transcript facilitates rescue of a plant rhabdovirus. Virol J 14:113.
7. Jackson AO, Li Z. 2016. Developments in plant negative-strand RNA virus reverse genetics. Annu Rev Phytopathol 54:469-98.
8. Desbiez C, Chandeysson C, Lecoq H, Moury B. 2012. A simple, rapid and efficient way to obtain infectious clones of potyviruses. J Virol Methods 183:94-7.
9. Chikh Ali M, Said Omar A, Natsuaki T. 2011. An infectious full-length cDNA clone of potato virus Y(NTN-NW), a recently reported strain of PVY that causes potato tuber necrotic ringspot disease. Arch Virol 156:2039-43.
10. Bedoya LC, Daros JA. 2010. Stability of Tobacco etch virus infectious clones in plasmid vectors. Virus Res 149:234-40.

11. Flatken S, Ungewickell V, Menzel W, Maiss E. 2008. Construction of an infectious full-length cDNA clone of potato virus M. Arch Virol 153:1385-9.
12. Bordat A, Houvenaghel MC, German-Retana S. 2015. Gibson assembly: an easy way to clone potyviral full-length infectious cDNA clones expressing an ectopic VPg. Virol J 12:89.
13. Lindbo JA. 2007. TRBO: a high-efficiency tobacco mosaic virus RNA-based overexpression vector. Plant Physiol 145:1232-40.
14. Boyer JC, Haenni AL. 1994. Infectious transcripts and cDNA clones of RNA viruses. Virology 198:415-26.
15. Dolja VV, McBride HJ, Carrington JC. 1992. Tagging of plant potyvirus replication and movement by insertion of beta-glucuronidase into the viral polyprotein. Proc Natl Acad Sci U S A 89:10208-12.
16. Mardanova ES, Kotlyarov RY, Kuprianov VV, Stepanova LA, Tsybalova LM, Lomonosoff GP, Ravin NV. 2015. Rapid high-yield expression of a candidate influenza vaccine based on the ectodomain of M2 protein linked to flagellin in plants using viral vectors. BMC Biotechnol 15:42.
17. Dickmeis C, Fischer R, Commandeur U. 2014. Potato virus X-based expression vectors are stabilized for long-term production of proteins and larger inserts. Biotechnol J 9:1369-79.
18. Tian J, Pei H, Zhang S, Chen J, Chen W, Yang R, Meng Y, You J, Gao J, Ma N. 2014. TRV-GFP: a modified Tobacco rattle virus vector for efficient and visualizable analysis of gene function. J Exp Bot 65:311-22.
19. Sempere RN, Gomez P, Truniger V, Aranda MA. 2011. Development of expression vectors based on pepino mosaic virus. Plant Methods 7:6.
20. Stevens M, Viganó F. 2007. Production of a full-length infectious GFP-tagged cDNA clone of Beet mild yellowing virus for the study of plant-polerovirus interactions. Virus Genes 34:215-21.
21. Rabindran S, Dawson WO. 2001. Assessment of recombinants that arise from the use of a TMV-based transient expression vector. Virology 284:182-9.
22. Zhao Y, Hammond J, Tousignant ME, Hammond RW. 2000. Development and evaluation of a complementation-dependent gene delivery system based on cucumber mosaic virus. Arch Virol 145:2285-95.
23. Shivprasad S, Pogue GP, Lewandowski DJ, Hidalgo J, Donson J, Grill LK, Dawson WO. 1999. Heterologous sequences greatly affect foreign gene expression in tobacco mosaic virus-based vectors. Virology 255:312-23.
24. Chapman S, Faulkner C, Kaiserli E, Garcia-Mata C, Savenkov EI, Roberts AG, Oparka KJ, Christie JM. 2008. The photoreversible fluorescent protein iLOV outperforms GFP as a reporter of plant virus infection. Proc Natl Acad Sci U S A 105:20038-43.
25. Wang Q, Ma X, Qian S, Zhou X, Sun K, Chen X, Jackson AO, Li Z. 2015. Rescue of a Plant Negative-Strand RNA Virus from Cloned cDNA: Insights into Enveloped Plant Virus Movement and Morphogenesis. PLoS Pathog 11:e1005223.
26. Ganesan U, Bragg JN, Deng M, Marr S, Lee MY, Qian S, Shi M, Kappel J, Peters C, Lee Y, Goodin MM, Dietzgen RG, Li Z, Jackson AO. 2013. Construction of a Sonchus yellow net virus minireplicon: a step toward reverse genetic analysis of plant negative-strand RNA viruses. J Virol 87:10598-611.
27. Hoenen T, Feldmann H. 2017. Reverse Genetics Systems for Filoviruses. Methods Mol Biol 1602:159-170.
28. Yoneda M, Guillaume V, Ikeda F, Sakuma Y, Sato H, Wild TF, Kai C. 2006. Establishment of a Nipah virus rescue system. Proc Natl Acad Sci U S A 103:16508-13.
29. He B, Paterson RG, Ward CD, Lamb RA. 1997. Recovery of infectious SV5 from cloned DNA and expression of a foreign gene. Virology 237:249-60.

30. Jackson AO, Dietzgen RG, Goodin MM, Li Z. 2018. Development of Model Systems for Plant Rhabdovirus Research. Adv Virus Res 102:23-57.
31. Neumann G, Watanabe T, Ito H, Watanabe S, Goto H, Gao P, Hughes M, Perez DR, Donis R, Hoffmann E, Hobom G, Kawaoka Y. 1999. Generation of influenza A viruses entirely from cloned cDNAs. Proc Natl Acad Sci U S A 96:9345-50.
32. Neumann G, Kawaoka Y. 1999. Genetic engineering of influenza and other negative-strand RNA viruses containing segmented genomes. Adv Virus Res 53:265-300.
33. Yamauchi Y (ed). 2018. Influenza Virus Methods and Protocols. Springer Science, New York, NY.
34. Mielke-Ehret N, Muhlbach HP. 2012. Emaravirus: a novel genus of multipartite, negative strand RNA plant viruses. Viruses 4:1515-36.
35. Waliczek T, Byrne D, Holeman D. 2018. Opinions of Landscape Roses Available for Purchase and Preferences for the Future Market. Hort Technology 28:807-14.
36. Pemberton H, Ong K, Windham M, Olson J, Byrne D. 2018. What is Rose Disease? HortScience 53:592-595.
37. McClellan M. 2017. Resisting Rose Rosette, vol May 2017, p 8-10. GIE Media, http://magazine.nurserymag.com/.
38. Cheng X, Deng P, Cui H, Wang A. 2015. Visualizing double-stranded RNA distribution and dynamics in living cells by dsRNA binding-dependent fluorescence complementation. Virology 485:439-51.
39. Okano Y, Senshu H, Hashimoto M, Neriya Y, Netsu O, Minato N, Yoshida T, Maejima K, Oshima K, Komatsu K, Yamaji Y, Namba S. 2014. In Planta Recognition of a Double-Stranded RNA Synthesis Protein Complex by a Potexviral RNA Silencing Suppressor. Plant Cell 26:2168-2183.
40. Bridgen A, Elliott RM. 1996. Rescue of a segmented negative-strand RNA virus entirely from cloned complementary DNAs. Proc Natl Acad Sci U S A 93:15400-4.
41. Debener T, Byrne DH. 2014. Disease resistance breeding in rose: current status and potential of biotechnological tools. Plant Sci 228:107-17.
42. Weber F, Wagner V, Rasmussen SB, Hartmann R, Paludan SR. 2006. Double-stranded RNA is produced by positive-strand RNA viruses and DNA viruses but not in detectable amounts by negative-strand RNA viruses. J Virol 80:5059-64.
43. Son KN, Liang Z, Lipton HL. 2015. Double-Stranded RNA Is Detected by Immunofluorescence Analysis in RNA and DNA Virus Infections, Including Those by Negative-Stranded RNA Viruses. J Virol 89:9383-92.
44. Rotenberg D, Thompson TS, German TL, Willis DK. 2006. Methods for effective real-time RT-PCR analysis of virus-induced gene silencing. J Virol Methods 138:49-59.

Figure Legends

FIG. 1. Successful mechanical inoculation of RRV.

(A) Image depicting the use of a hand-held artist airbrush to deliver sap inoculum to rose plants.

(B) RT-PCR verifies the presence of antigenomic RNA1, RNA3, RNA4, RNA5, RNA6, and RNA7 in inoculated *Arabidopsis* and *N. benthamiana*. Virus infected rose plants taken from field samples were used as a positive control in these experiments.

(C) Microscopic image showing the results of dsRBFC assay in mock treated and RRV infected *N. benthamiana* leaves. dsRBFC was carried out for fluorescence labelling RRV dsRNA replication intermediates. Scale bar is 50 µm.

FIG. 2. Diagrammatic representation of constructs**.**

Open boxes depict the coding region for each segment of the RRV genome. RNA segments 1 through 7 are identified on the left and the size of each segment is identified either inside the open box or on the right. GFP was introduced into RNA 4 as a direct fusion to the open reading frame creating RNA4-GFP. GFP was also fused to the foot and mouth disease virus 2a peptidase and fused to the RNA4 open reading frame to produce a self-cleaving polyprotein. All cDNAs of antigenomic viral RNAs were introduced into the binary plasmid pCB301 between the 35S promoter and hepatitis delta virus ribozyme.

FIG. 3. Two rose varieties infected with RRV1-7 infectious clone at 55 dpi.

(A and B) Mock inoculated and virus infected plants that produce deep pink flowers, of 'The Knock Out'® rose variety. Infected plants do not show symptoms and resemble the mock plants although they test positive for virus.

(C)Image of plants in the greenhouse showing healthy roses next to infected roses of 'The Double Knock Out'® variety. These infected plants show early signs of witch's broom.

(D-G) Images of infected 'The Double Knock Out'® plants with witch's broom. Necrosis on leaves and early buds. Leaves are small and round.

FIG. 4. *Arabidopsis* infected with RRV1-4 and RRV1-7.

(A) Images of mock treated, RRV1-4, and RRV1-7 infected plants taken at 45 dpi (68 days after germination). (B) RT-PCR produced 500 bp product, verifying accumulation of RNA4 transcripts in systemic leaves of *Arabidopsis* plants at 25 dpi. Actin primers were used for internal control amplification of 292 bp product, showing equal quantities of RNA in each lane. Final lane on the left is positive control sample from infected roses. (C) Images of inoculated leaves taken at 24 dpi (D, E) Inflorescences of mock treated and RRV1-4 infected plants at 45

dpi. Infected plants show larger cauline leaves and more branches. (F-H) Images of basal and aerial rosettes on plants infected with RRV1-7 at 45 dpi.

FIG. 5. *N. benthamiana* infected with RRV1-4 and RRV1-7.

(A, B) Images of mock treated and RRV1-4 infected plants at 25 dpi.

(C) Image of mock, RRV1-4 and RRV1-7 infected plants taken at 20 dpi shows mild symptoms compared to previous experiment in panels A and B.

(D) RT-PCR verified accumulation of RNA1 through RNA4 in two samples of *N. benthamiana* (lanes 1, 2) and control rose samples (lanes 5, 6). Two mock control samples were included (lanes 3, 4). RNA segments are identified on the left. The amplicon sizes are identified on the right of each ethidium bromide stained 1.2% agarose gel.

(E) Multiple RT-PCR using three RNA samples from plants infected with RRV1-4 (lanes 2-4) and three samples from RRV1-7 (lanes 5-7). One RNA sample from mock treated plants (M, lane 1) was included. Amplicons representing each RNA1 through 7 are identified on the right. Narrow arrows point to individual products while the block arrow identifies the aggregate of bands representing RNAs3-7 which co-migrate on a gel. The "*" identifies intermediate size amplicons as reported in Babu et al (2016).

(F) RNAse protection assay detecting double-stranded RNAs. Total RNAs were treated with DNAse I and then treated with 0, 1, and 5 units (U) of RNase I to digest single-strand RNA, leaving dsRNA intact. RT-PCR amplification is carried out using same primers as in panel D and listed in Table 1. Products were analyzed by 1.2% agarose gel electrophoresis. The RNAs 1 through 4 are identified on the left and size of each amplicon is indicated on the right. L= 1kb ladder.

FIG. 6. *N. benthamiana* infected with 4R4-GFP and 7R4-GFP.

(A) Introduced GFP into RNA4 fusing the coding region with the RRV RNA4 open reading frame (P4) creating the R4-GFP construct. Plants were inoculated with RRV RNAs1-4 with R4-GFP (named 4R4-GFP) or with RRV RNAs1-7 with R4-GFP (7R4-GFP). Plants showed necrosis on systemic leaves in young and mature plants.

(B) Microscopic imaging shows GFP expression in 4R4-GFP and 7R4-GFP leaves. Scale bars = 100 µm.

(C) Immunoblot detects ~70 kDA GFP-P4 fusion protein in plants inoculated with 4R4-GFP or 7R4-GFP. The mock sample is identified in lane 0. Membranes were stained with Ponceau S or Coomassie blue to verify equal loading of samples.

(D) RT-PCR diagnostic using agRRV4-F1/R1 primer set to identify infected samples. Lane 1 in each gel is no reverse transcript control added to PCR reaction, and lane 2 is RNA from mock treated sample. Lanes 3-6 are virus infected samples. PCR primers detecting EF1 as internal control.

(E) RT-PCR was carried out using 5 µg of total RNA for each sample to verify the presence of genomic and antigenomic RNA1, RNA3, RNA4, RNA5, RNA6, and RNA7 in inoculated *Arabidopsis* and *N. benthamiana*. Virus infected rose plants taken from field samples were used as a positive control in these experiments.

FIG. 7. *N. benthamiana* infected with 4R2-iLOV, 7R2-iLOV and 7R5-iLOV.

(A) Diagrammatic representation of iLOV fused to ORF2 on RNA2 and introduced into RNA5 replacing the ORF5.

(B) Images of plants at 25 dpi that are mock inoculated or systemically infected with RRV 4R2-iLOV and 7R2-iLOV. Epifluorescence microscope images of infected leaves at 13 dpi shows fluorescence in epidermal cells. Bars= 100 µm.

(C) Images of plants at 25 and 35 dpi that are mock inoculated or systemically infected with RRV 7R5-iLOV. Epifluorescence microscope images of infected leaves at 13 dpi shows fluorescence in epidermal cells. Bars= 100 µm.

(D) RT-PCR diagnostic using agRRV4-F1/R1 primer set to identify infected samples. PCR primers detecting EF1 as internal control showing equal loading in each lane. L=1 kb ladder.

(E) RT-PCR detecting each viral segment identified on the left. Samples infected with 4R2-iLOV, 7R2-iLOV and 7R5-iLOV are identified above the gels. EF-1 is a control PCR showing equal loading in each lane.

Supplemental Fig 1.

RT PCR detection of each RRV segment using RNA from systemically infected leaves. Lane 1 is mock (M), lanes 2 and 3 are Knockout® roses, and lanes 4 and 5 are Double Knockout® roses.

Table 1 Total proportion of systemically infected plants confirmed at 25 dpi by RT PCR using agRRV4 F1/R1 primer set

Constructs	*Arabidopsis*	*N. benthamiana*	Knock Out® roses	Double Knock Out® roses
Rose sap inoculated plants[a]	13/18	12/12		
Buffer treated[a]	0/8	0/8		
pCB301[b]	0/12	0/12	1/4	4/4
RRV1-7[b]	11/12	17/18	12/12 [d]	7/8 [d]
RRV1-4[b]	10/12	16/18		
RRV1-4GFP[b]	5/12	21/21		
RRV1-7GFP[b]	6/12	21/21		
4R2-iLOV		8/8		
7R2-iLOV		8/8		
7R5-iLOV		8/8		
RRV1-7-Nb sap inoculated plants[c]	2/6			
Buffer treated plants alongside RRV1-7-Nb sap inoculated plants[c]	0/3			

[a] The proportion of infected *Arabidopsis* plants were pooled from two experiments and the proportion of infected *N. benthamiana* were from one experiment.

[b]The proportion of infected *Arabidopsis* plants were pooled from three experiments and the proportion of infected *N. benthamiana* were pooled from two experiments. Rose plants have been prescreened for no infected ones for further infectious clone treatments. All plants were assayed by RT-PCR at 25 dpi

[C] The proportion of Arabidopsis plants that were identified at 25 dpi to be infected following inoculation with sap taken from RRV1-7 *N. benthamiana* plants (also at 25 dpi) or buffer.

[d] Knock Out® roses, can detect RRV infection in new emerging leaves at 30 dpi and in double knockout detects 40 dpi.

Table 2 Infection characteristics in Arabidopsis

	pCB301 mock	**RRV seg 1-4**	**RRV seg 1-7**
Inflorescence emergence (days)	59	45	45
Proportion of total plants with lateral inflorescence branches	2/4	6/6	6/6
Proportion of total plants with secondary inflorescence branches	2/4	6/6	6/6
Proportion of total plants with tertiary inflorescence branches	0/4	6/6	6/6
Proportion of total plants with aerial Rosettes	3/4 have <10 aerial rosettes	6/6 have >30 aerial rosettes	6/6 have >40 aerial rosettes
Average Height	22.0 cm	51.0 cm	45.0 cm
Average Number of Siliques/plant	50 (short)	250 (long)	200 (long)
1000 seed weight	16 mg	17 mg	18 mg
Seed germination	100%	100%	100%

Representative data from one experiment collected from 4 mock treated plants and 6 RRV infected plants for each category.

A

B

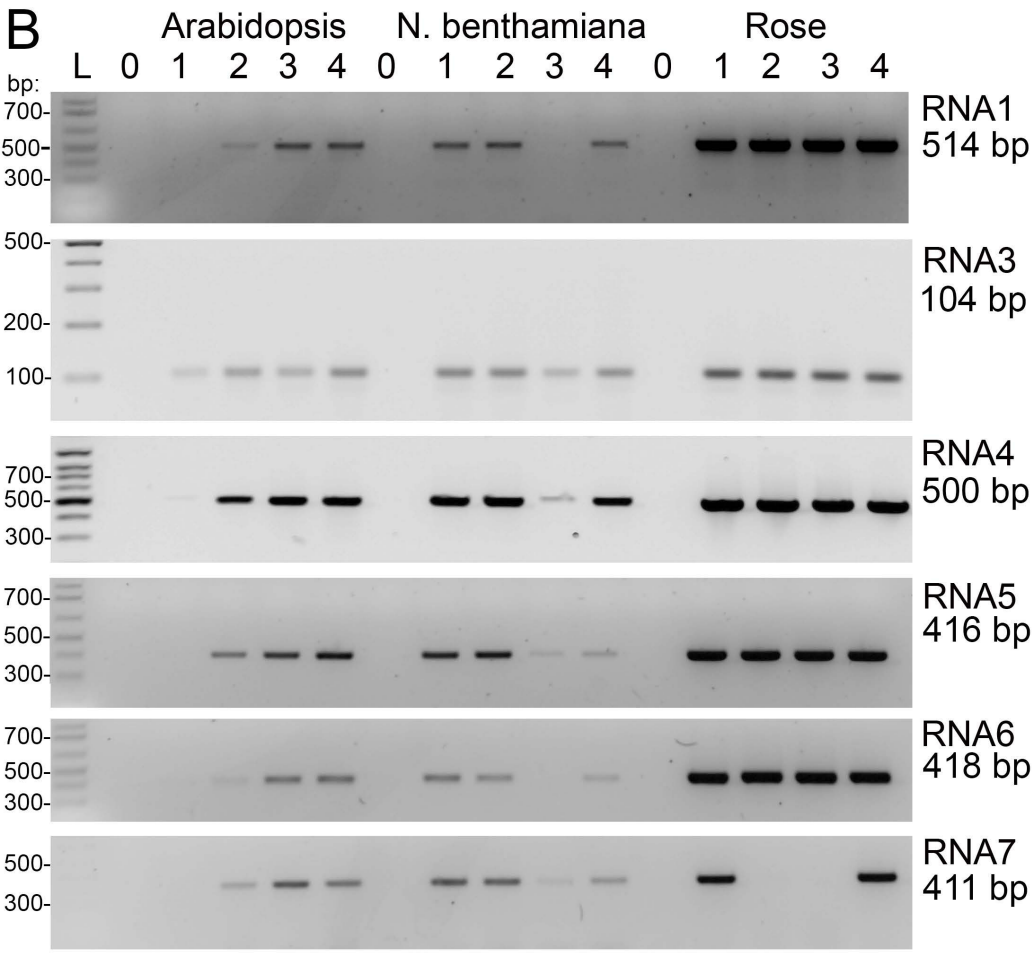

C

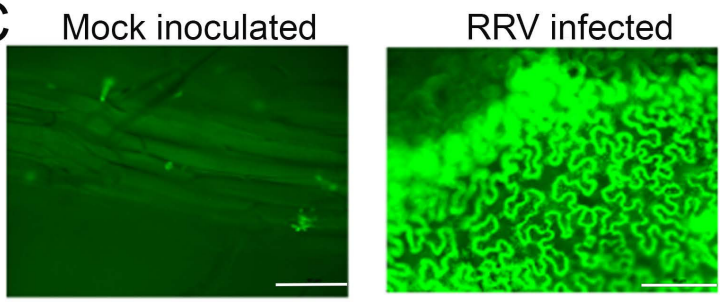

Figure 1

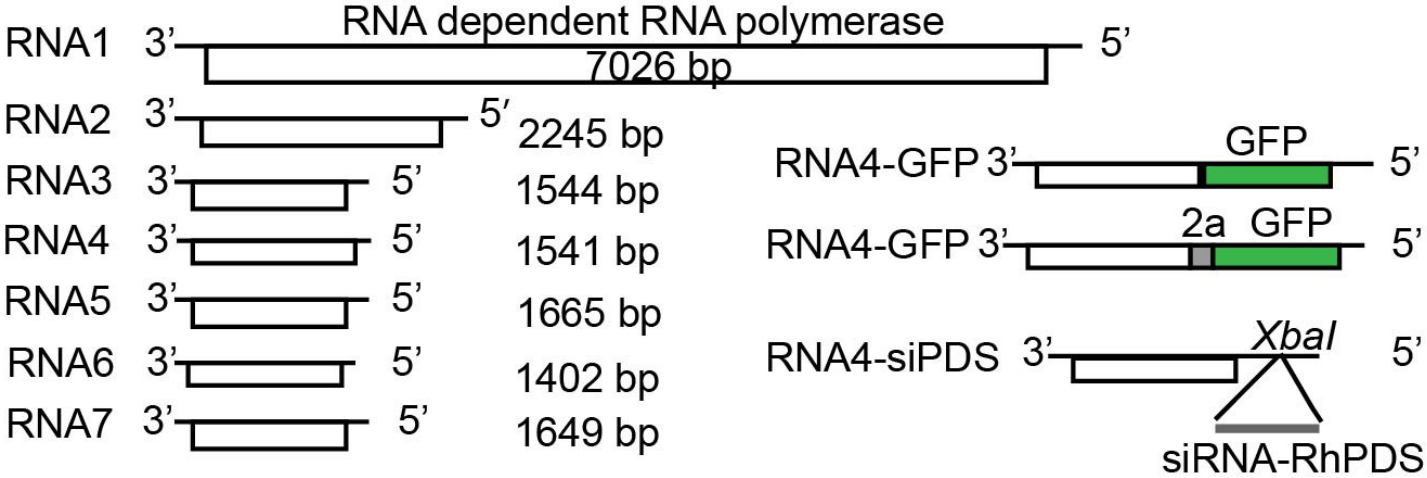

Binary plasmid pCB301

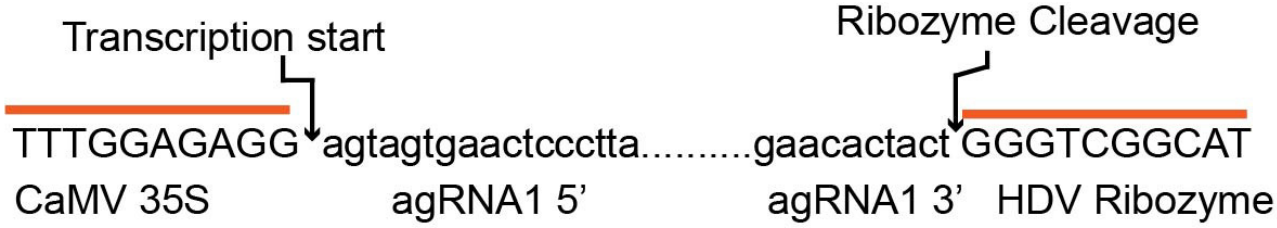


A
Mock (Knockout Roses)
B
Inf (Knockout Roses)
C
Healthy
Inf (Double knockout)
D
Inf (Double Knockout)
E
Inf (Double Knockout)
F
Inf (Double Knockout)
G
Inf (Double Knockout)

Figure 3

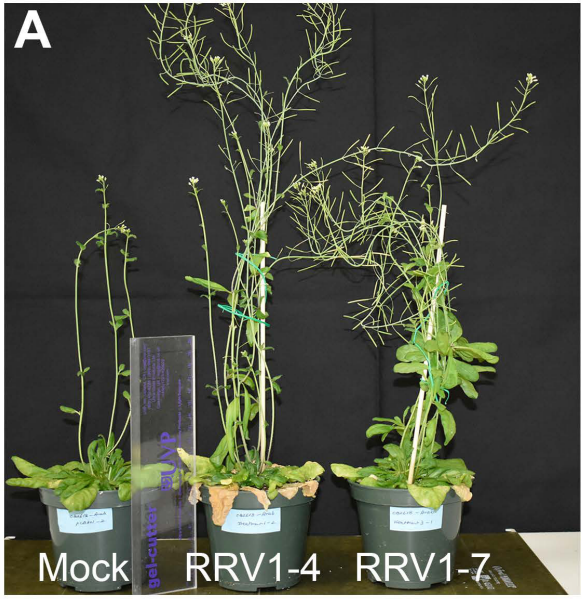

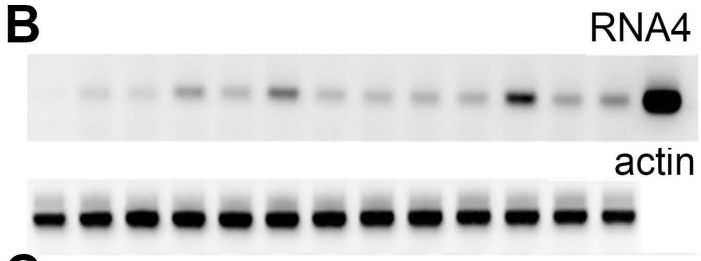

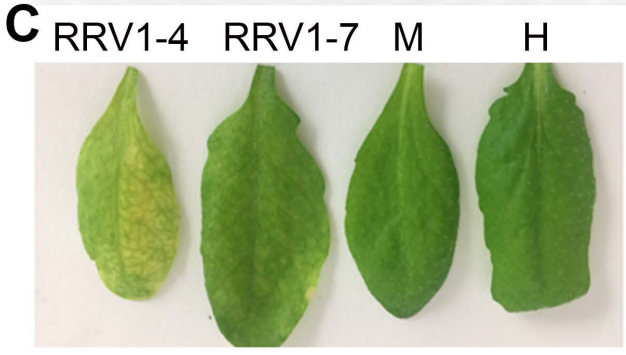

Figure 4

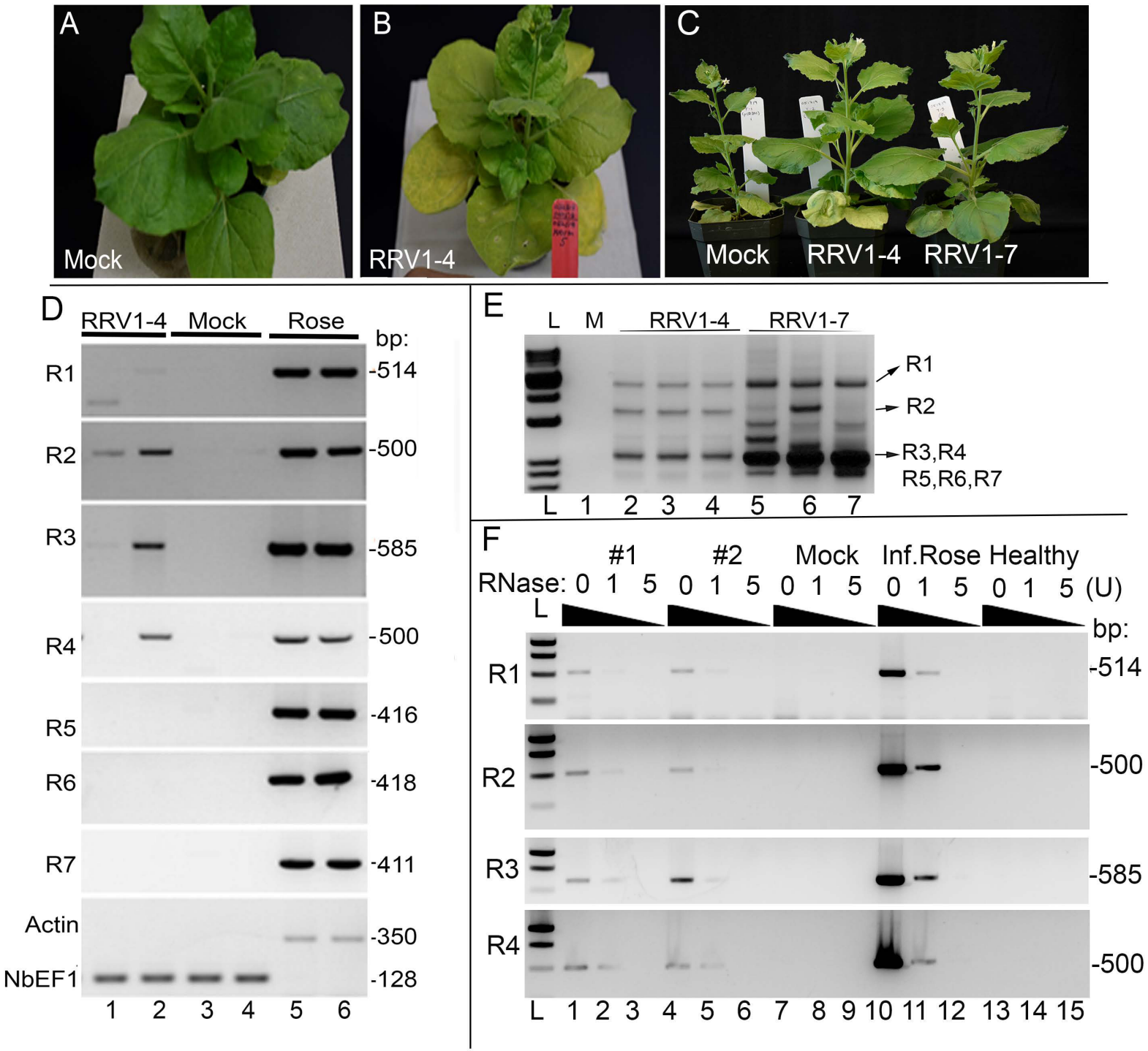
A
Mock
B
RRV1-4
C
Mock
RRV1-4
RRV1-7
D
RRV1-4
Mock
Rose
bp:
R1
-514
R2
-500
R3
-585
R4
-500
R5
-416
R6
-418
R7
-411
Actin
-350
NbEF1
-128
1 2 3 4 5 6
E
L M
RRV1-4
RRV1-7
R1
R2
R3,R4
R5,R6,R7
L 1 2 3 4 5 6 7
F
#1
#2
Mock
Inf.Rose
Healthy
RNase: 0 1 5 0 1 5 0 1 5 0 1 5 0 1 5 (U)
L
bp:
R1
-514
R2
-500
R3
-585
R4
-500
L 1 2 3 4 5 6 7 8 9 10 11 12 13 14 15

Figure 5

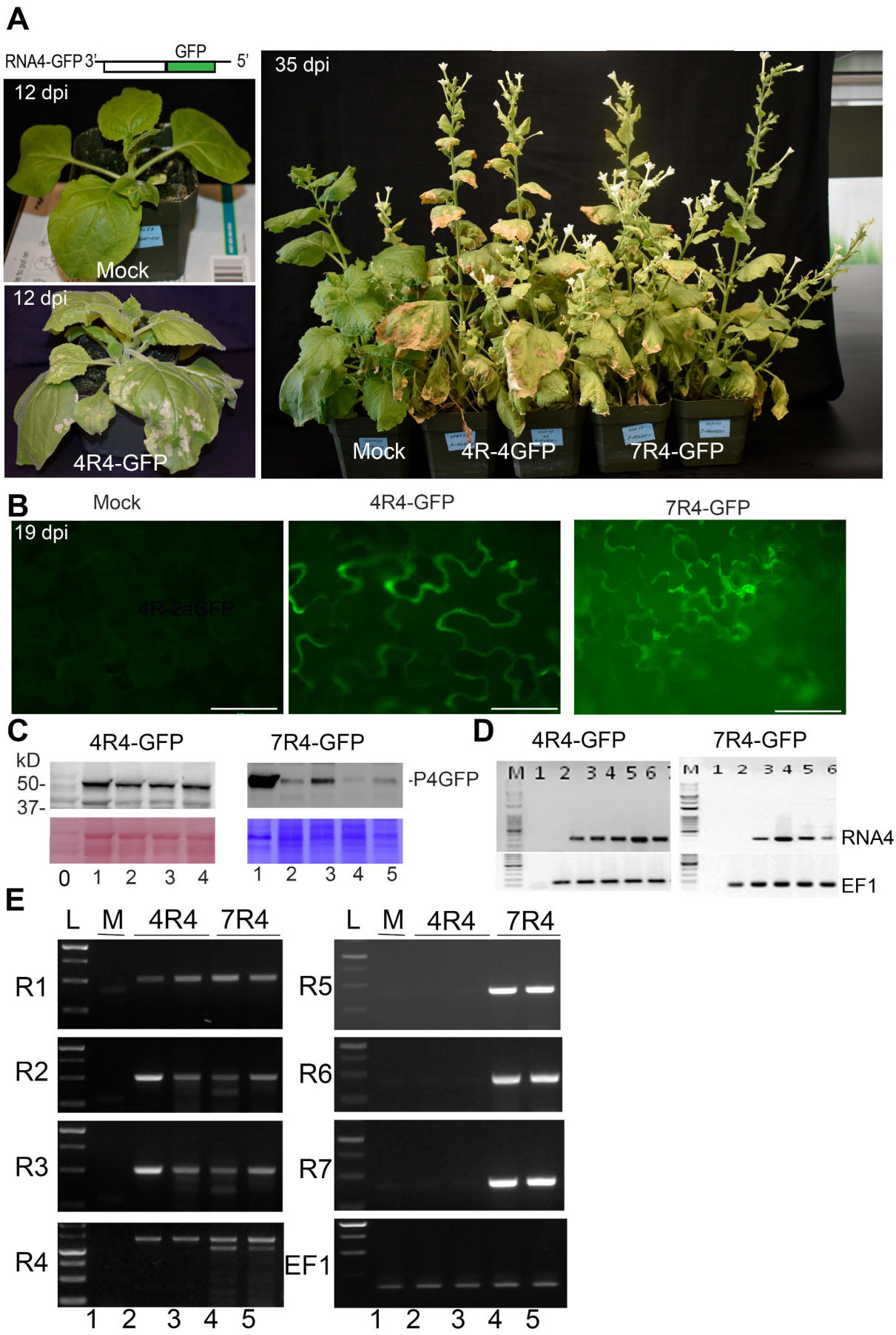

Figure 6

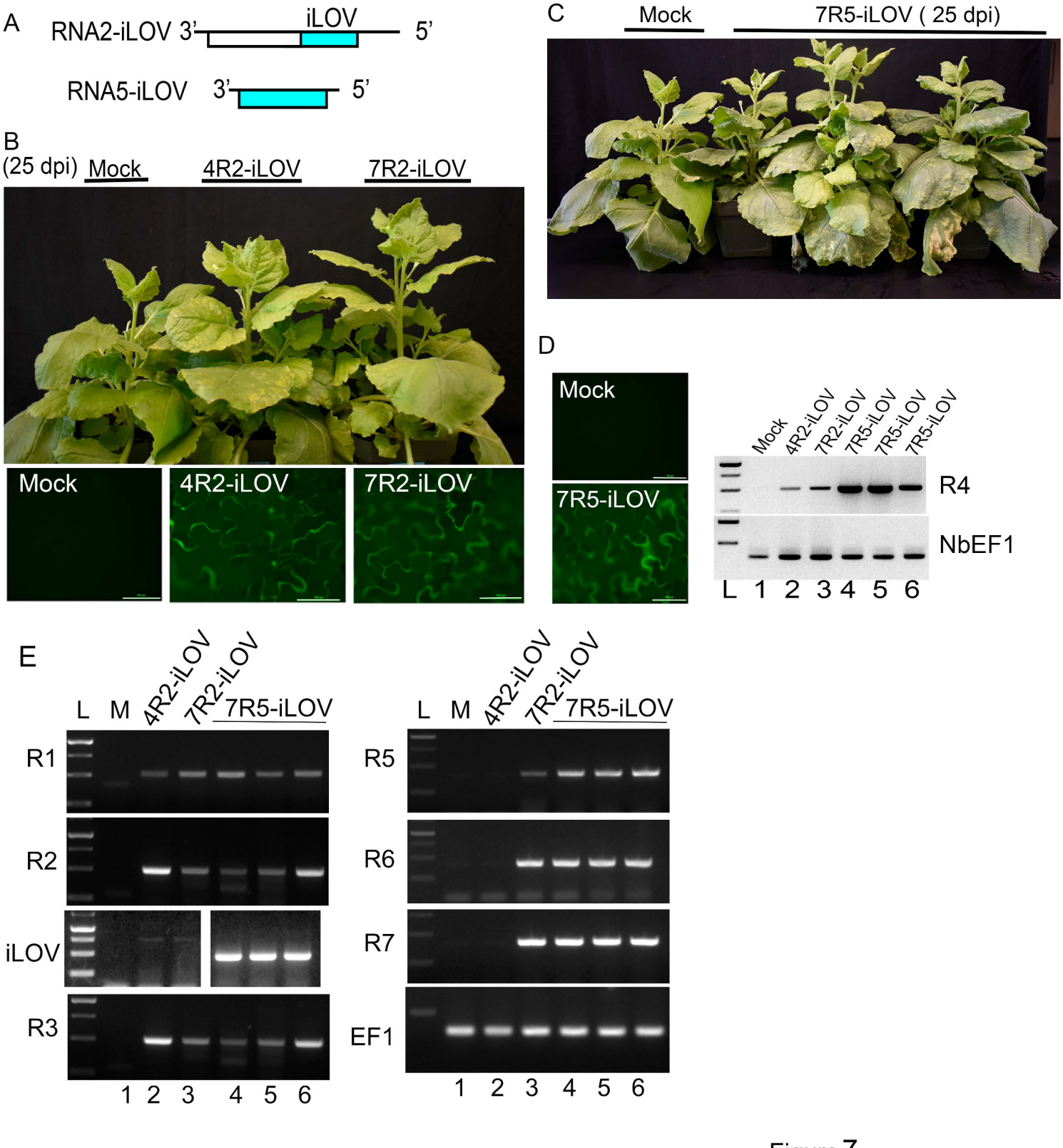
A
RNA2-iLOV 3'
iLOV
5'
RNA5-iLOV
3'
5'
B
(25 dpi)
Mock
4R2-iLOV
7R2-iLOV
Mock
4R2-iLOV
7R2-iLOV
C
Mock
7R5-iLOV (25 dpi)
D
Mock
7R5-iLOV
Mock
4R2-iLOV
7R2-iLOV
7R5-iLOV
7R5-iLOV
7R5-iLOV
R4
NbEF1
L 1 2 3 4 5 6
E
L M 4R2-iLOV 7R2-iLOV 7R5-iLOV
R1
R2
iLOV
R3
1 2 3 4 5 6
L M 4R2-iLOV 7R2-iLOV 7R5-iLOV
R5
R6
R7
EF1
1 2 3 4 5 6

Figure 7